

# Seismic reflection studies of the Amery Ice Shelf, East Antarctica: delineating meteoric and marine ice

Kathleen L. McMahon and Mark A. Lackie

Department of Earth and Planetary Sciences, Macquarie University, North Ryde, NSW, 2109 Australia. E-mail: kcmahon@els.mq.edu.au

Accepted 2006 April 20. Received 2006 April 11; in original form 2004 November 15

## SUMMARY

A detailed seismic reflection survey has been performed, utilizing a 24-channel spread with a 10 m geophone spacing, giving a maximum fold coverage of six, with the aim of revealing a detailed view of the subsurface structure of the Amery Ice Shelf, showing meteoric and marine ice thicknesses, water column thickness and sediment structure. The survey has successfully delineated the subhorizontal meteoric and marine ice layers, with average thicknesses of 754 and 20 m, respectively. The water column is 595 m thick, placing the seafloor at a depth of 1369 m below the ice surface. A 55 m thick, subhorizontally layered sedimentary unit can be seen, below which are deep features, at approximately 2225 m below the surface. These features could reveal the presence of dykes, a broken bedrock surface or glaciologically derived clasts that are sufficiently large enough to show up within the data.

**Key words:** Amery Ice Shelf, East Antarctica, ice shelf, marine ice, reflection seismology, refraction seismology.

## INTRODUCTION

The Amery Ice Shelf (AIS) is located on the east coast of Antarctica, at approximately 70°S, 70°E (Fig. 1). It is the third largest embayed shelf in Antarctica, and the largest in East Antarctica (Allison 2003), and as such is one of the largest glacier drainage basins in the world. Due to this, and its thermal isolation, the AIS plays an important role in the global climate system (Allison 2003; Passchier *et al.* 2003). Knowing the structure of the AIS is important to studies of the impact of global warming on present-day ice shelves and the subsequent effect on global ocean circulation and climate (Allison 2003; Hemer & Harris 2003; Passchier *et al.* 2003). Understanding the structure of the AIS can also provide tighter control in mass balance calculations of the shelf and in ocean circulation models beneath the ice cover.

To date, the bathymetry, and hence the water column thickness, under the ice shelf is poorly known. What limited information there is available comes from about 80 seismic observations taken by the Soviet Antarctic Expedition (SAE) in the 1970s, none of these being taken south of 71°35'S (Hunter *et al.* 2004; Allison 2003). These gave the earliest indications of the depth of the ocean floor (Allison 2003), and presumably this Russian data has been used to help produce the bathymetry image and vertical section of the AIS as displayed in Hunter *et al.* (2004).

More recently, airborne ice radar data have been collected over the shelf (Allison 2003), but the results for these surveys are limited. Marine ice thicknesses for the AIS have been calculated using a digital elevation model (DEM) and airborne radio-echo soundings (RESs), assuming hydrostatic equilibrium for the shelf (Fricker *et al.*

2001). Due to the high absorption of electromagnetic energy by marine ice, ice radar will not penetrate into it (Blindow 1994), and hence ice radar is only useful to map the thickness of meteoric ice. Two ice cores have been taken on the front of the shelf as part of the Amery Ice Shelf Ocean Research (AMISOR) project (Craven *et al.* 2003), a project which aims to quantify the interaction between the ocean and the AIS, to determine the implications of this for the discharge of grounded ice and water mass modification, and to derive the long time record of the variability of this interaction (Allison 2003). The ice-radar method is based on indirect observations/data, and the hot-water drilling takes one expeditionary season to complete a single hole, since drilling through the ice shelf is only one step of a series of experiments they undertake. In reality, another quick, direct surveying technique is required to accurately map sections of the AIS.

The seismic geophysical technique is a powerful tool for surveying the thickness and structure of the subsurface, and this makes it suitable for the investigation of the structure of the AIS. A vast amount of data can be relatively quickly acquired, to reveal a complete picture of the subsurface in terms of ice, water and sediments.

Using seismic refraction and a detailed reflection survey, the main aim of the study was to map the thickness of both the ice and water column, hence depth to the seafloor, and most importantly to see if a delineation could be made between meteoric and marine ice. Meteoric and marine ice have different physical properties, such as density and elastic properties, meaning a seismic survey, if detailed enough, should be able to delineate the two boundaries. Such a survey may also reveal structure within the sediments, adding to knowledge of possible seafloor processes.

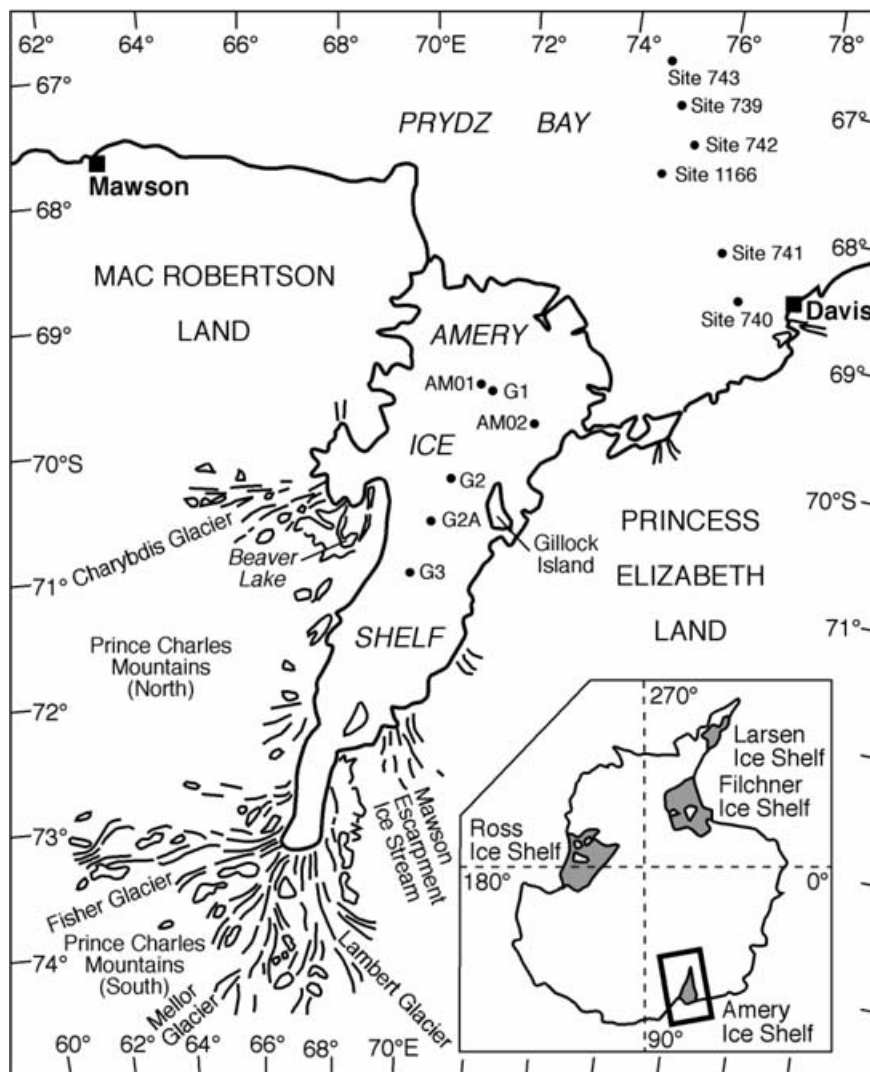


Figure 1. Map of the Amery Ice Shelf, East Antarctica. Inset: Map of Antarctica showing the major ice shelves.

## GLACIOLOGY

The AIS is formed from the convergence of the Lambert, Mellor, Fisher and Charybdis Glaciers, and the Mawson Escarpment Ice Stream (Fig. 1). It extends for approximately 550 km north of its grounding zone at 73.2°S (Fricker *et al.* 2002), and is bounded by the Prince Charles Mountains (PCMs), draining through the Lambert Graben, and emptying into Prydz Bay. The Lambert Glacier drainage basin is quite well defined by ice surface contouring. Flowlines that determine the surface slope were obtained using RES (Drewry 1983), showing the ice funnelling into the Lambert Graben.

The Lambert Graben is quite well defined by both seismic (Stagg 1985; Federov *et al.* 1982) and magnetic (Federov *et al.* 1982) data. It is about 100 km wide and extends south for approximately 700 km, displaying a bedrock relief of up to 3500 m, which is mainly overlain by ice (Federov *et al.* 1982). Magnetic data shows depressions in the basement, up to 5 km in depth, filled with nonmagnetic rocks.

Ice thickness is variable and tends to smooth the underlying topography (Hambrey 1991). Ice is thinnest at the coast, with a thickness less than 500 m and some areas of bare rock being exposed. It is also thin in areas of higher elevation, such as the PCMs, where rock

is exposed as nunataks. In the Lambert Graben below the Mawson Escarpment ice is 2500 m thick, the thickness decreasing with distance north to about 900 m at the AIS's grounding line and 270 m at the shelf front. In all other areas, the ice becomes thicker inland to a maximum of about 3000–3500 m at the margins of the drainage basin.

The topography of the floor of Prydz Bay is characterized by a deepening coastward from about 500 m at the continental shelf break to over 1000 m in some places near the coast, forming what is known as the Amery Basin (Hambrey 1991). This is also known as the Amery Depression (Phil O'Brien, private communication, 2005), being a depression which sits on top of the Prydz Bay Basin, a sedimentary basin. From the front of the AIS, the Amery Basin deepens progressively to the south under the ice shelf and the Lambert Glacier, reaching a depth of at least 2500 m below sea level (Hambrey 1991).

Previous glaciological research sites where detailed data were acquired on the AIS are G1 (69.5°S, 71.5°E) about 60 km from the shelf front, G2 and G3 (Fig. 1). At these sites, ice cores, density and temperature data, as well as ice velocity measurements were collected and ice thickness was found using radar (Allison 2003).

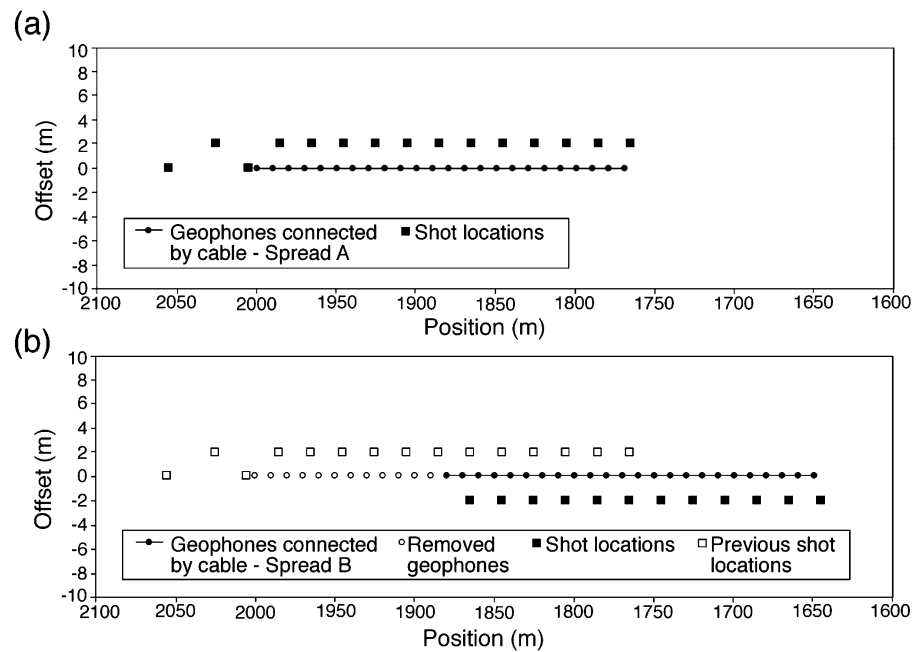


**Figure 2.** Method employed for shifting the reflection survey: (a) Geometry of the first spread (south end of line); (b) Geometry of the second spread. Seven of these overlapping spreads were surveyed in total. The orientation of the line was  $083^\circ$  magnetic.

## GEOLOGY

In MacRobertson Land and Princess Elizabeth Land (Fig. 1) nearby the AIS, exposed rock are widespread in the PCMs. Geochronological investigations by Australian geologists suggested lower grade rocks exposed in the southern PCMs to be of Archaean age and the highest grade rocks to be of late Proterozoic age (Tingey 1982).

The Archaean crystalline basement underlies an area of about  $130\,000\text{ km}^2$  of the AIS–PCM region, and is up to 20 km thick (Ravich & Federov 1977). Proterozoic metasedimentary rocks occupy an area approximately 200 km by 100 km in the southern PCMs, with a thickness of 7 to 8 km (Tingey 1972).

After the Early Palaeozoic Pan-African orogeny (Mikhalsky *et al.* 2001), tectonic activity in the area was dominated by crustal-block movement, resulting in a longitudinal system of horsts and narrow depressions. One of these is the Beaver Lake graben, where Permian coal-bearing, flat lying deposits are preserved. They directly overlie the strongly eroded crystalline basement (Ravich 1974), having a total area of outcrop of  $450\text{ km}^2$  (Hambrey 1991) and an observable thickness of 1300 m (Ravich & Federov 1977). Despite the relatively small outcrop of Permian and younger rocks, Hambrey (1991) believed much of the AIS region is underlain by such sediments, especially in the complex Lambert Graben structure under the Lambert Glacier–AIS system.

## METHODOLOGY

The surveys were carried out near G2A (Fig. 1) in the middle of the AIS, the southern-most geophone of the line being located at  $70^\circ 33.5'S$ ,  $70^\circ 20.6'E$ . A 24-channel spread was used with a 10 m geophone spacing, the line oriented at bearing  $083^\circ$  magnetic ( $010^\circ$  true), to orientate the line approximately parallel to the direction of flow. A Geometrics Strataview R48 seismograph was used, located at the centre of the spread. Groups of four 14 Hz geophones were used for every channel, to improve the signal-to-noise ratio

(SNR). These were placed in  $\sim 30$  cm deep holes to keep them out of the wind and snow drift, and were spaced up to 10 cm apart, in the cross-line direction. For the reflection survey, the source consisted of two Pentax H boosters (150 g) and a single Nobel 35 g primer. The source depth was 2 m, which was cored using a Polar Ice Coring Office (PICO) corer. For the refraction survey, the exterior shots utilized a Nobel 35 g primer and the centre shot an Orca No 8 electrical detonator. The source depth was 1 m for the primers and 10 cm for the detonators.

### Refraction survey

This survey was carried out to detail the shallow surface structure and to find a seismic velocity for ice near the surface. Two refraction surveys were completed at the southern and northern ends of the detailed reflection survey line. Shot locations for the refraction surveys were at 25 m and 1 m exterior to the line, and also a central shot. All were on-line with the spread, using an explosive source.

### Reflection survey

The detailed reflection line was surveyed in between and inclusive of the refraction lines. We could not perform a roll-along reflection survey, since we did not have suitable cables, so to overcome these limitations, geophone spreads were moved in sections to maintain fold coverage, maximum six, over the entire line. Walk on shots were taken at 55, 25 and 5 m exterior to the spread, and interior shots were taken every 20 m (Fig. 2a). The 25 m exterior shot was offset 2 m since that online location had already been used for a refraction shot. The spread was moved north by 12 geophones so that the new Channel 1 was at the old Channel 13 location (Fig. 2b). Shots needed to be repeated at the same locations, so for different spreads shots were offset 2 m alternatively to the east or west of the line. In total, seven spreads were completed. Using this method, 89 shots were taken in total to cover a line distance 1.06 km.

## PROCESSING

Refraction data were processed using the Seismic Refraction Interpretation Programs (SIP) v4.1 (Rimrock Geophysics) and RAY-INVR (Zelt & Smith 1992) programs. A three-layer model was plotted to represent snow, semi-compacted snow and ice. Reflection data were processed using two software packages—Seismic Unix (SU) (Colorado School of Mines) and GLOBE Claritas<sup>©</sup> v3.3.0 (Claritas<sup>©</sup>) (New Zealand Institute for Geological and Nuclear Sciences).

The raw reflection data were of an overall good quality, with high-amplitude refraction data dominating the upper part of the records, persisting until approximately 400 ms in the data. All reflections appear as approximately horizontal reflections, arriving at approximately 400, 800, 1250, 1650 and 2030 ms.

The data were first converted to SU seg-y format then to Claritas<sup>©</sup> seg-y format. All 89 shot records were formed into a single file and field geometry was applied. Data quality was improved by trace editing, including front muting to remove refracted arrivals, and trace deletion to remove individual noise traces. Ranges of maximum frequency gained from performing a spectral analysis were used to construct a bandpass frequency domain filter to remove high-frequency noise.

A preliminary velocity analysis gave a velocity of  $2500 \text{ m s}^{-1}$  for a pre-stack NMO correction. The data were then sorted according to common depth point (CDP) number (numbered 100–301 going from south to north), and the CDP geometry file was applied. The CDP sorted data were then stacked. True stacking velocities (using a simple three-layer model representing ice, water and sediments) were found to be  $3300 \text{ m s}^{-1}$  for the ice/water reflection set and  $3080 \text{ m s}^{-1}$  for the water/sediment reflection set. Automatic gain control (AGC) and balancing were performed on the data, however, they produced no improvement in the data, and in the case of the AGC, made interpretation more difficult, and so neither were used for the final stack.

## RESULTS

### Refraction

The refraction data revealed a three-layer structure of snow, semi-compacted snow (firn) and ice. An example of a SIP time–depth conversion model from the refraction data is shown in Fig. 3(a). The surface snow layer varied from 3–5 m thick and the firn displayed a variable thickness, but had an average of about 20 m. This variability of the firn/ice boundary may be due to the change not being such a definite boundary, but more gradational. The average seismic velocity of the ice layer taken from nearby surface refraction surveys is  $3545 \pm 158 \text{ m s}^{-1}$ , and the highest measured value is  $3710 \text{ m s}^{-1}$ . When a model with a gradational increase in density (and hence seismic velocity) of the firn layer is undertaken using ray tracing (Fig. 3b), then the thickness of the firn layer is about 40 m with a seismic velocity increasing from  $\sim 2100 \text{ m s}^{-1}$  at the top of the layer to  $\sim 3700 \text{ m s}^{-1}$  at the bottom.

### Reflection

The stacked reflection data (Fig. 4a) clearly show two major reflection sets. The first shows two definite reflections at 397 ms and 404–411 ms, with multiples of these occurring at 390 ms intervals. The upper reflector can be interpreted as the base of the meteoric ice,

and the lower reflector as the base of the marine ice (Fig. 4b). The thickness in two-way time (TWT) of the marine ice layer becomes 12 ms at CDP 100, decreasing to 7 ms between CDP 125 and 301. The time difference locally increases to about 10 ms around CDP 175.

The second reflection set is from the water/sediment boundary. The sediments show at least four persistent reflection boundaries, starting at approximately 1240, 1276, 1306 and 1337 ms taken from the reflection times at CDP 100. The earliest reflection time in the record for the first sediment reflection is 1227 ms. This reflection set has multiples at 387 ms intervals down the record (Fig. 4a). The primary sediment reflection boundaries all occur at  $\sim 30$  ms intervals, which implies that the lower three reflections are more likely reverberations from internal reflections than true primary reflections, meaning they are intrabed multiples. The reverberations appear to be exact copies of the first arrival sediment reflection. The duration of the true primary sediment reflection within the record is, therefore, 26 ms.

Well below the sedimentary layering in the stack, discrete hyperbolic reflections can be seen (Fig. 4a). Referring to these hyperbolae by the CDP number of their uppermost point, the five hyperbolae occur at CDP 107, 130, 137, 225 and 267. The earliest arrival is 1679 ms at CDP 107, and the latest is 1955 ms at CDP 225.

## DISCUSSION

The seismic data shows two major reflection sets; the ice/water boundary and the water/sediment boundary. There are two reflections in the ice/water boundary; the upper reflection is interpreted as the base of the meteoric ice, and the lower as the base of the marine ice.

The ice/water boundary reflections seem similar in the record, both in time arrival and the time difference between them. This leads to the question of whether the lower reflection is simply a ghost from the free surface of the upper reflection. Hand picking the times for the meteoric/marine–ice boundary and the marine–ice/water boundary shows that the two reflections are parallel for 46 per cent of the CDP values and show inverse (reverse polarity) characteristics for 54 per cent of the CDP traces. Assuming a ghost would turn up as a reflection of reverse polarity, this would show that the entire reflection is not a ghost. Time differences in the parts of the gather that show reverse polarity are not constant, compared within or between these areas of reverse polarity. Since all shot depths were the same, this also does not concur with ghosting. If the second reflection was a ghost, it would be expected the average of the arrival times be a straight line between the two. This is not the case, and so the second reflection by all indications seems to be a true reflection and not simply a ghost of the first.

Refraction surveys at the ends of the detailed line give velocities for the top 3 m of snow of  $851 \pm 19 \text{ m s}^{-1}$  for the south end, and  $1094 \pm 288 \text{ m s}^{-1}$  for the north. Taking account of errors, the maximum range of velocity for snow on the line is  $806\text{--}1382 \text{ m s}^{-1}$ . Similar velocities were also found from refraction lines surveyed 500 m to the south of the detailed line. Over a distance of 2 m for a shot, these velocities for snow would add a time delay of 2.8–4.8 ms to the reflection arrival. For a depth of 2.5 m (the maximum shot–depth possible) the time delay added is 3.6–6.2 ms. With the measured time difference between the first and second reflection generally being 7–13 ms, and the average being 9.8 ms, these calculated delay times are well below what is seen in the data. If we use this actual time difference of 9.8 ms with the known shot depth to calculate a

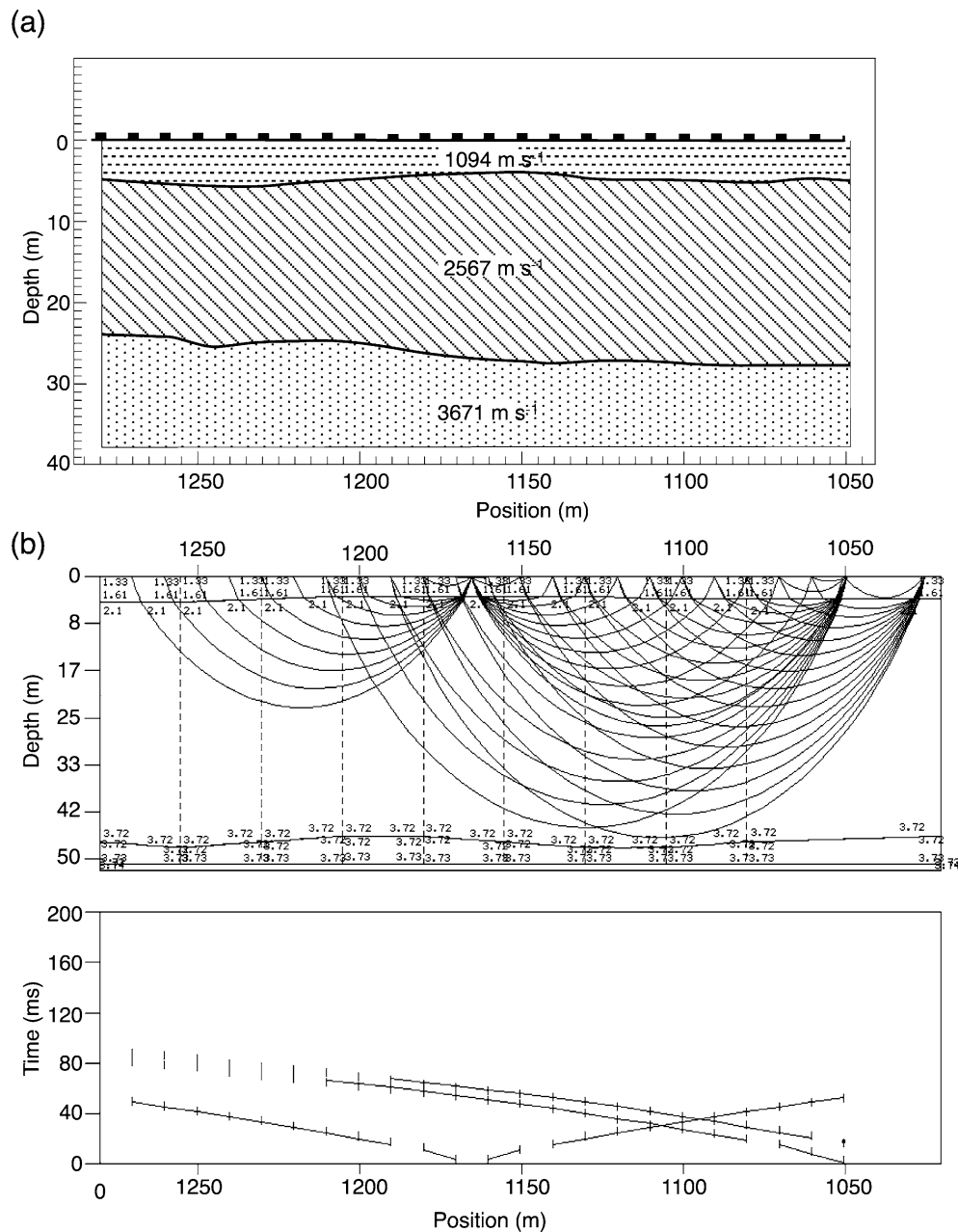


**Figure 3.** (a) Time–depth conversion of the refraction data from the northern end of the detailed reflection line. Geophone locations are shown on the top of the image. Velocities are given within the layers in  $\text{m s}^{-1}$ . (b) Inverse ray-tracing model of the same line. Internal upper and lower boundary velocities are given in  $\text{km s}^{-1}$ .

velocity, the velocity of the surface layer would have to be as low as 408–510  $\text{m s}^{-1}$  for the signal to be a ghost, which is below the lowest velocities found from refraction processing of all data in the area. All this suggests the reflections are not ghosting, but actual reflections of two definable boundaries.

In order to compare these results with previous studies, the arrival times of reflections were converted into depths (Fig. 5). Reasonable near-surface seismic ice velocities were gained from the seismic refraction data. Seismic ice velocities can also be calculated using the density and temperature of the ice (Robin 1958, cited in Thiel & Ostenso 1961). The closest density and temperature readings of the ice shelf is at G1, located about 130 km downstream (to the north) of G2A, where temperature and density profiles have been taken

(Budd *et al.* 1982; Mike Craven, private communication, 2003). In other Antarctic ice shelves, seismic ice velocities have also been calculated, for example, the maximum velocity of ice of the Ross Ice Shelf (RIS) is 3839  $\text{m s}^{-1}$  (Thiel & Ostenso 1961). Considering the calculations from density and temperature, and the refraction results, a seismic velocity that could represent the entire ice layer is 3800  $\text{m s}^{-1}$ . This was used to calculate the thickness of both the glacial and marine ice, with a maximum error of  $\pm 50 \text{ m s}^{-1}$  in the velocity. The error of picks for the time arrivals is up to 2 ms. However, this is the maximum error, and in most cases the arrivals could be picked to within 0.5 ms accuracy. The thickness of the meteoric ice, therefore, is  $754 \pm 4 \text{ m}$ , and the marine ice varies from 13–27 m thick, with an error in the range 4–8 m.

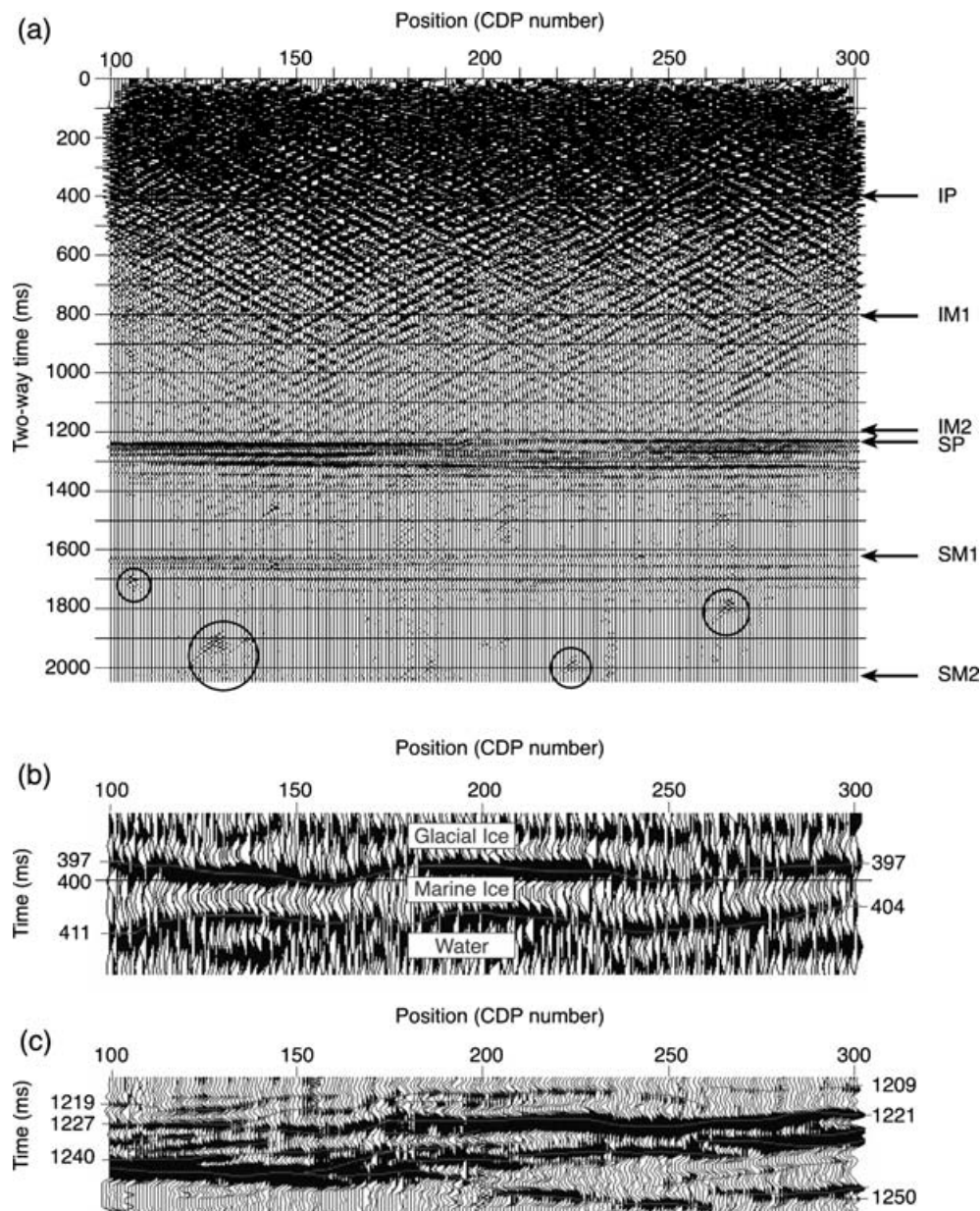


**Figure 4.** (a) CDP stacked section of processed reflection data showing all major reflections. Legend: IP—primary ice reflection; IM1—first-order ice multiple; IM2—second-order ice multiple; SP—primary sediment reflection; SM1—first-order sediment multiple; SM2—second-order sediment multiple. Circled objects are the deep hyperbolic reflections. (b) Detailed image of ice boundaries, with interpretation. (c) Detailed image of sedimentary layering, with interpretation.

The thickness of the water column can be calculated using a seismic velocity between  $1400$  and  $1500$   $\text{m s}^{-1}$ . Cochrane & Cooper (1991) used a seismic velocity of  $1460$   $\text{m s}^{-1}$  for the Prydz Bay water column, based on temperature and salinity measurements made at the Prydz Bay drill sites, whereas Beaudoin *et al.* (1992) used a velocity of  $1440$   $\text{m s}^{-1}$  on the RIS. Cochrane & Cooper's (1991) value is the closer in proximity to the AIS, however, the environmental setting must be taken into account. The  $1460$   $\text{m s}^{-1}$  value for Prydz Bay is based on the specific temperature and salinity measurements taken in Prydz Bay ocean waters. Under the AIS, there would be mixing of fresh water with the saline sea water from the melting of the shelf itself. Therefore, it would have a lower salinity, and a different seismic velocity. Beaudoin *et al.*'s (1992) value,  $1440$   $\text{m s}^{-1}$ , has been proposed for the water under the RIS, and

taking this as indicative of Antarctic waters under ice shelves, this velocity was used to calculate the water column thickness of the AIS. The water column thickness ranges from  $597$  m at the south end of the line to  $594$  m in the north, the average thickness being  $595$  m. This places the seafloor at a depth below the surface ranging from  $1378$  to  $1362$  m, from south to north.

Glacial material under the RIS has a seismic velocity of  $2700$   $\text{m s}^{-1}$  (Beaudoin *et al.* 1992; Parasnis 1997; Sharma 1997), and sediment thickness under the ice shelf was calculated using this value (Beaudoin *et al.* 1992). Sonobuoy seismic studies in Prydz Bay taken on ODP Leg 119 show near surface seismic velocities exceed  $2000$   $\text{m s}^{-1}$  at all sites studied (Cochrane & Cooper 1991). The data collected at Sonobuoy 5 (at Site 740; see Fig. 1), the closest to the AIS, show a range of seismic velocities for the glacial sediments

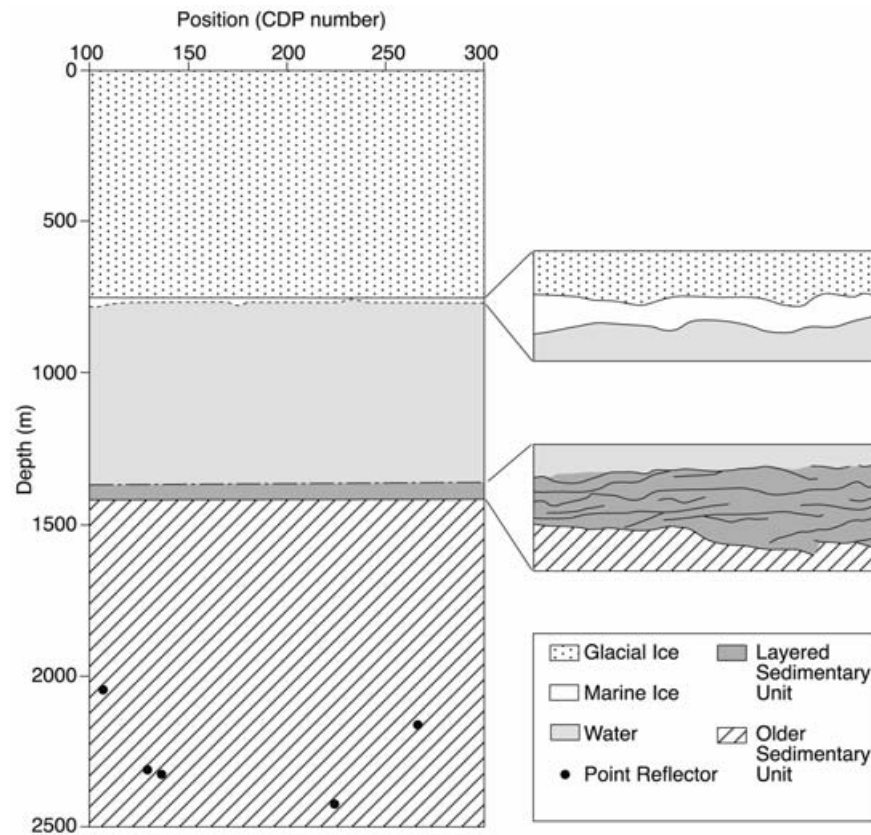


**Figure 5.** A converted depth model of the reflection data, showing enlargements of the glacial/marine-ice boundary and sedimentary layering.

between  $\sim 2300$  and  $2850 \text{ m s}^{-1}$ . This supports the use of  $2700 \text{ m s}^{-1}$  as a seismic velocity for the glacial sediments under the AIS. The AIS being in a similar environment with glacial sediments, a velocity of  $2700 \text{ m s}^{-1}$  has been used to calculate the thickness of this sedimentary column, which gives the stratified sedimentary sequence a thickness of 51–58 m. Using the full range of velocities ( $2300\text{--}2850 \text{ m s}^{-1}$ ) and a picking error of less than 0.5 ms to gain an idea of the error in this value, the thickness maybe be a maximum of 10 m thinner, or 5 m thicker. The point reflectors have also had depths calculated using  $2700 \text{ m s}^{-1}$  as the velocity, since there is no indication that the overlying materials have changed from a glacial type. These occur at depths ranging from approximately 2020 to 2400 m, with the average depth being approximately 2225 m.

The thicknesses of the ice and ocean cavity as modelled by Hunter *et al.* (2004) agree with the results we have obtained at G2A, and with previous depths measured from actual core data taken at site AM01 (near G1) (Fig. 1). In a bathymetry image of the AIS produced by Hunter *et al.* (2004) (produced in part from the sparse 1970s SAE seismic data), the depth to the seafloor in the image around our survey area is anywhere from 1100 to 1800 m in depth. The depth we found at G2A is well within this range. The thickness of ice under our survey location according to the profile produced by Hunter *et al.* (2004), extracted from the above-mentioned bathymetry image, is about 700 m, with no delineation given between meteoric and marine ice. The seafloor boundary in the profile is at about 1375 m below the surface. The depths gained from our survey relate well to these values, and can be used to support the models produced by Hunter *et al.* (2004).

From the AIS marine ice thickness models produced by Fricker *et al.* (2001), the marine ice thickness at our survey location is

$\sim 20\text{--}30$  m. This model is in good agreement with what is seen in the seismic data, where the marine ice thickness varies from 13–27 m. Fricker *et al.* (2001) model can also be compared to studies at G1, including a 315 m drill core taken in 1969 (Budd *et al.* 1982). This core revealed a three-layer structure in the AIS, with the marine ice being 45 m thick starting at a depth of 270 m (Allison 2003). Morgan (1972) used oxygen isotope evidence to show that the thickness of the shelf at G1 is 428 m thick, as determined by ice radar, and this results in a marine ice thickness of 158 m. Fricker *et al.* (2001) have given the thickness of marine ice here to be  $141 \text{ m} \pm 30 \text{ m}$ , which is consistent with Morgan's (1972) value. Fricker *et al.*'s (2001) model can then be considered as a robust image of the marine ice beneath the AIS.

The sediments under our survey line, as defined by seismic reflections, can be interpreted in terms of bedding (Fig. 4c). Individual beds are of approximately 3 ms thickness in TWT. The sedimentary layering shows evidence of sedimentary processes. The two major amplitude boundaries seen in the reflections decrease in amplitude to either end of the record—the upper reflection loses amplitude to the south, whereas the major reflection below that decreases in amplitude to the north, which may indicate a possible sedimentary foreset. The sediment reflections also reveal structures such as truncated beds (Fig. 4c, Fig. 5). Structures such as this have been described in sediments under other ice shelves and in glacial environments (Eyles & Eyles 1992; Lachniet *et al.* 1999; Raunholm *et al.* 2002).

It may be that the  $\sim 55$  m of stratified sediments seen in our seismic data are unconsolidated, and below these are more massive (hence non-reflection producing) and/or more compacted sedimentary units

that could be as old as the Oligocene or Eocene (Cochrane & Cooper 1991; Ehrmann 1991). In Prydz Bay, sedimentary units have been identified, including diatomaceous clay, diamictites, sands and carbonaceous shales, Lower Cretaceous sandstones and silts, and red bed sandstones and siltstones (Cochrane & Cooper 1991; Cooper *et al.* 1991; Stagg 1985). The bedrock under these sedimentary units, in Prydz Bay and under the AIS, is most likely Meso- to Early Neoproterozoic (Precambrian) high-grade metamorphic rocks (Cooper *et al.* 1991; Mikhalsky *et al.* 2001), based on mapping of the nearby PCMs.

The sediments taken from AM02 (Fig. 1) show lodgement till at the base of the core sample (Hemer & Harris 2003). Lodgement till is deposited closest to the grounding zone of the glacier, and is commonly compact with oriented clasts (Bennett & Glasser 1997; Drewry 1986; Sugden & John 1976). Till generally contains a large amount of erratic material, and so the point reflectors may be large boulders.

The point reflectors are seen quite distinctly in the raw data, and do not appear to be a relict of processing, but a true feature. Upon analysis of every raw record, the hyperbolic reflections do appear in numerous records at approximately the correct position as where they would appear in the CDP gather. They do not appear in every record, but consistently enough for the existence of something at depth producing these hyperbolae to be a definite possibility. They are not simply caused by shot-generated noise, since they do not show the same characteristic as this type of event, which is a persistent high-amplitude anomaly throughout the record for two to three traces around the shot location. Also, the hyperbolae are found in the record unrelated to shot location.

When comparing the times and positions of the significant hyperbolae seen in the stacked record to times and positions of hyperbolae in the individual records, there is a remarkable correlation. Times in the records closely, and sometimes almost exactly, match arrivals in the stacked section.

From the hyperbola reflection shapes in the stacked section, whatever is responsible would appear to be inclined to the south, except for the one at CDP 107, which seems to be more vertical than the others. However, in the raw records, the hyperbolae appear to be more symmetric. The inclination could be due to the stacking process.

The hyperbolae could represent the presence of boulders, which would fit a glacial environment of deposition, possibly from a time when the grounding zone of the AIS was further north, dropping large boulders within the till. Hyperbolic point reflections could indicate vertical fractures (broken bedrock) or a blocky, bouldery texture—the result of basal ice structures from the glaciation that deposited the sediments (Sweat 1997). In the case of our data, it is possible that the point reflectors indicate a broken or jagged bedrock surface. Assuming the AIS was grounded somewhere nearby in its past, the action of the ice working on the bedrock could have deformed the substrate, as happens in glacial environments (Eyles & Eyles 1992), producing this kind of surface. The absence of any linear reflection between the individual hyperbolae in the data, however, means it cannot be confidently stated that the hyperbolae indicate a bedrock surface.

Other surveys performed in the region of the AIS suggest that the bedrock could appear in the data record (Federov *et al.* 1982). According to a cross-section through the AIS based on geophysical data, especially deep seismic sounding (Federov *et al.* 1982), the bedrock begins at a depth of  $\sim 1$  km. Mishra *et al.* (1999), who studied the gravity and magnetic anomalies of the Lambert Graben, also mention that the bottom of the subglacial valley is greater than 1 km below sea level. Fricker *et al.* (2001) states the AIS sits in a

long, narrow cavity with a maximum draft of 2200 m. This depth is also approximately coincident with the depth where the point reflectors appear. If the glaciers were once grounded further north than where they are at present, features could be evident at this same depth, again meaning the hyperbolae are possibly related to features produced by basal glacier processes.

The Ocean Drilling Program (ODP) Leg 188, discussed by Passchier *et al.* (2003), took drill cores in Prydz Bay. The closest drill site to the shelf is Site 1166, located approximately 400 km from the front of the ice shelf on the continental shelf, where drilling penetrated 343 m of Holocene through to Cretaceous sediments. A seismic interpretation of the extent and depth of the sediments shows that they are around 670 m deep. If the depth of hyperbolic point reflections under G2A indicate a bedrock surface, and the material above that, is therefore, sediment deposits, to an approximate thickness of 835 m, this would indicate a much larger thickness of sediments in the ice shelf cavity than in the open sea.

A 225.5 m sediment core was retrieved from Site 740, showing sandstones and siltstones overlain by diatom ooze (Hambrey *et al.* 1991). The seismic line ODP-119, part of ODP Leg 119, was surveyed over Sites 739, 742, 741, and 740 (Fig. 1). It shows basement rock, most likely eroded Precambrian metamorphic rock, occurs to depths of up to 2 km, and probably deeper (Cooper *et al.* 1991; Federov *et al.* 1982). Magnetic profiles that have been taken across Prydz Bay show there is a minimum basement depth of 2.5–3 km (Cooper *et al.* 1991). This shows a similar depth as our data, so again this suggests the possibility that bedrock is seen under the glacial units in our data.

Another possible cause for the deep hyperbolic reflections is the presence of dykes within the basement. An eroded surface in which dykes display higher relief than surrounding weathered softer material could form a terrain that would produce the results we have seen. In effect, the dykes would be a relatively narrow ridge, acting like a point for the seismic waves to reflect off, producing a hyperbola in the seismic record. The difference in physical properties alone of the dykes compared to their host rock may also be sufficient to produce the hyperbolic reflections.

The most likely rocks to be found under G2A are those belonging to the Beaver-Lambert Terrane, as described by Mikhalsky *et al.* (2001). Within the Beaver-Lambert Terrane are found mafic granulite, ultramafic and metadolerite dykes, mostly 2–15 m wide, with some material gathering in small plutons up to 50 m across (Mikhalsky *et al.* 2001). These types of dykes may be what our detailed reflection survey has imaged.

## CONCLUSION

The seismic survey employed on the AIS to produce a detailed image of the subsurface structure has been successful. Using a geophone spacing of 10 m, with 20 m spaced interior shots to maintain a six fold coverage, a seismic data set has been produced that has revealed detailed information about the AIS subsurface. In particular it has imaged the marine ice layer, which up to now, beside time-consuming drill core sampling, had only been imaged using numerical modelling, such as Fricker *et al.*'s (2001) method utilizing RESs and DEMs. It is extremely important to note the seismic technique's ability to directly view the marine ice itself.

The detailed reflection data collected in this survey on the AIS has revealed a detailed view of the subsurface structure, clearly delineating the meteoric and marine ice boundaries, defining a water column thickness, and sedimentary structure with the upper 55 m



of sediments. The marine ice layer ranges in thickness from 13 to 27 m, and the 55 m of stratified sediments show structures such as truncated beds and foresets. The part of the record below this unit that displays no reflections is likely formed of massive sandstones or siltstones (Hambrey *et al.* 1991), and compared to sediments off the front of the shelf, they could possibly be as old as Oligocene in age (Ehrmann 1991). Point reflectors seen at ~2200 m depth are in most likelihood features of a broken bedrock surface (the result of glacial action), large boulders or the presence of dykes. This bedrock surface refers to older Proterozoic rocks, whereas above this would be the Permian–Tertiary sediments (Hambrey 1991). The depth to this surface found from our data correlates with estimated depths made by Federov *et al.* (1982) and Fricker *et al.* (2001), and bedrock depths gained from reflection data off the front of the ice shelf (Cooper *et al.* 1991).

Detailed seismic studies make a valuable accompaniment to current GPS and drill core studies on the AIS. It overcomes the problems encountered with ice radar where the marine ice cannot be seen, and improves upon the SAE seismic data where the marine ice was also not mapped. So overall, the method for seismic studies on the AIS as used for this study is a useful method for mapping the subsurface structure of the AIS in a quick, easy to repeat manner, and would be beneficial in a continuation of studies on the AIS.

The bathymetry, and hence the water column thickness, under the AIS is poorly known up to this date (Hunter *et al.* 2004), and performing more surveys such as this seismic survey would greatly improve the quantity and quality of data gathered on the AIS, providing clarification on the current structural model of the AIS. A better model means improvements can be made to mass balance calculations, and any change of the mass balance can be better recorded and analysed. This in turn will improve studies of global climate change, and how this affects the volume of ice in Antarctica and fluctuations in global sea level.

## ACKNOWLEDGMENTS

Thanks go to Richard Coleman (University of Tasmania), Jeremy Bassis (SCRIPPS Institute), Alan Elcheikh (AAD), Michael Woolridge (AAD) and Chris Legge (AAD), for their assistance in the collection of data. Also to Phil O'Brien, Tim Barton, and Alan Crawford of Geoscience Australia for generously supplying seismic equipment for the survey, and to ANARE for their logistical support. Phil O'Brien and an anonymous reviewer are thanked for their constructive reviews, which have resulted in an improved manuscript. This research was funded by ASAC Project 2542. This is contribution 430 from the ARC National Key Centre for Geochemical Evolution and Metallogeny of Continents (GEMOC).

## REFERENCES

- Allison, I., 2003. The AMISOR project: ice shelf dynamics and ice-ocean interaction of the Amery Ice Shelf. Forum for Research into Ice Shelf Processes, Report (14). Web address: <http://www.gfi.uib.no/frisp/Rep14/allison.pdf> (accessed 15/06/05)
- Beaudoin, B.C., ten Brink, U.S. & Stern, T.A., 1992. Characteristics and processing of seismic data collected on thick, floating ice: results from the Ross Ice Shelf, Antarctica, *Geophysics*, **57**(10), 1359–1372.
- Bennett, M.R. & Glasser, N.F., 1997. *Glacial geology, ice sheets and landforms*, p. 364, John Wiley & Sons, New York, NY.
- Blindow, N., 1994. The central part of the Filchner-Ronne Ice Shelf, Antarctica: internal structures revealed by 40 Hz monopulse RES, *Ann. Glaciol.*, **20**, 365–371.
- Budd, W., Corry, M.J. & Jacka, T.H., 1982. Results from the Amery Ice Shelf Project, *Ann. of Glaciol.*, **3**, 36–41.
- Cochrane, G.R. & Cooper, A., 1991. Sonobuoy seismic studies at ODP drill sites in Prydz Bay, Antarctica, in *Proceedings of the Ocean Drilling Program, Scientific Results*, Vol. 119, pp. 27–43, eds Barron, J., Enderson, J., Baldauf, J. & Larsen, B.
- Cooper, A., Stagg, H. & Geist, E., 1991. Seismic stratigraphy of Prydz Bay, Antarctica: implications from Leg 119 drilling, in *Proceedings of the Ocean Drilling Program, Scientific Results*, Vol. 119, pp. 5–25, eds Barron, J., Enderson, J., Baldauf, J. & Larsen, B.
- Craven, M., Elcheikh, A., Brand, R. & Allison, I., 2003. Hot water drilling on the Amery Ice Shelf, East Antarctica. Forum for Research into Ice Shelf Processes, Report (14). Web address: <http://www.gfi.uib.no/frisp/Rep14/craven.pdf> (accessed 15/06/05)
- Drewry, D.J. (Ed.), 1983. *Antarctica: Glaciological and Geophysical Folio*, Scott Polar Research Institute, Cambridge.
- Drewry, D.J., 1986. *Glacial Geologic Processes*, 1st edn, pp. 132–133, Edward Arnold Ltd., London.
- Ehrmann, W.U., 1991. Implications of sediment composition on the southern Kerguelen Plateau for paleoclimate and depositional environment, in *Proceedings of the Ocean Drilling Program, Scientific Results*, Vol. 119, pp. 185–210, eds Barron, J., Enderson, J., Baldauf, J. & Larsen, B.
- Eyles, N. & Eyles, C., 1992. Glacial depositional systems, in *Facies Models: Response to Sea Level Change*, pp. 73–100, eds Walker, R.G. & James, N.P., Geological Association of Canada.
- Federov, L.V., Grikurov, G.E., Kurinin, R.G. & Masolov, V.N., 1982. Crustal structure of the Lambert Glacier from geophysical data, in *Antarctic Geoscience*, pp. 931–936, eds Craddock, C., Loveless, J.K., Vierima, T.L. & Crawford, K., University of Wisconsin Press, Madison, Wisconsin.
- Fricker, H.A., Popov, S., Allison, I. & Young, N., 2001. Distribution of marine ice beneath the Amery Ice Shelf, *Geophys. Res. Lett.*, **28**(11), 2241–2244.
- Fricker, H.A. *et al.*, 2002. Redefinition of the Amery Ice Shelf, East Antarctica, grounding zone, *J. geophys. Res.*, **107**(B5), ECV 1/1–1/9.
- Hambrey, M.J., 1991. Structure and dynamics of the Lambert Glacier-Amery Ice Shelf system: implications for the origin of Prydz Bay sediments, in *Proceedings of the Ocean Drilling Program, Scientific Results*, Vol. 119, pp. 61–74, eds Barron, J., Enderson, J., Baldauf, J. & Larsen, B.
- Hambrey, M.J., Ehrmann, W.U. & Larson, B., 1991. Cenozoic glacial record of the Prydz Bay Continental Shelf, East Antarctica, in *Proceedings of the Ocean Drilling Program, Scientific Results*, Vol. 119, pp. 77–132, eds Barron, J., Enderson, J., Baldauf, J. & Larsen, B.
- Hemer, M. & Harris, P.T., 2003. Sediment core from beneath the Amery Ice Shelf, East Antarctica, suggests mid-Holocene ice-shelf retreat, *Geology*, **31**(2), 127–130.
- Hunter, J., Hemer, M. & Craven, M., 2004. Modeling the circulation under the Amery Ice Shelf. Forum for Research into Ice Shelf Processes, Report (15). Web address: <http://www.gfi.uib.no/frisp/Rep15/hunter.pdf> (accessed 15/06/05)
- Lachniet, M.S., Larson, G.J., Strasser, J.C., Lawson, D.E., Evenson, E.B. & Alley, R.B., 1999. Microstructures of glacial sediment-flow deposits, Matanuska Glacier, Alaska, in *Glacial processes: past and present*, pp. 45–57, eds Mickelson, D.M. & Attig, J.W., Boulder, Colorado, Geological Society of America Special Paper 337.
- Lønne, I., 1995. Sedimentary facies and depositional architecture of ice-contact glaciomarine systems, *Sediment. Geol.*, **98**, 13–43.
- Mikhalsky, E.V., Sheraton, J.W., Laiba, A.A., Tingey, R.J., Thost, D.E., Kamenev, E.N. & Federov, L.V., 2001. Geology of the Prince Charles Mountains, Antarctica. AGSO—Geoscience Australia, Canberra; bulletin 247.
- Mishra, D.C., Chandra Sekhar, D.V., Venkata Raju, D. Ch. & Vijaya Kumar, V., 1999. Crustal structure based on gravity-magnetic modelling constrained from seismic studies under Lambert Rift, Antarctica and Godavari and Mahanadi rifts, India and their relationship, *Earth planet. Sci. Lett.*, **172**(3–4), 287–300.
- Morgan, V.I., 1972. Oxygen isotope evidence for bottom freezing on the Amery Ice Shelf, *Nature*, **238**(5364), 393–394.

- Parasnis, D.S., 1997. *Principles of applied geophysics*, 5th edn, Chapman & Hall, London.
- Passchier, S., O'Brien, P.E., Damuth, J.E., Januszczak, N., Handwerker, D.A. & Whitehead, J.M., 2003. Pliocene-Pleistocene glaciomarine sedimentation in eastern Prydz Bay and development of the Prydz Bay trough-mouth fan, ODP Sites 1166 and 1167, East Antarctica, *Mar. Geol.*, **199**, 279–305.
- Raunholm, S., Larsen, E. & Sejrup, H.P., 2002. Weichselian sediments at Foss-Eikeland, Jæren (southwest Norway): sea level changes and glaciation history, *J. Quat. Sci.*, **17**(3), 241–260.
- Ravich, M.G., 1974. Section through the Permian coal measures in the Beaver Lake area (Prince Charles Mountains, East Antarctica), *Antarktika, Doklady Komissii*, **13**, 19–35.
- Ravich, M.G. & Federov, L.V., 1977. Geologic structure of MacRobertson Land and Princess Elizabeth Land, East Antarctica, in *Antarctic Geoscience*, pp. 499–504, eds Craddock, C., Loveless, J.K., Vierima, T.L. & Crawford, K., University of Wisconsin Press, Madison, Wisconsin.
- Robin, G. deQ., 1958. Seismic shooting and related investigations: Norwegian-British-Swedish Antarctic Expedition, 1949–1952, Scientific Results. V5, Norsk Polarinstitut, Oslo.
- Sharma, P.V., 1997. *Environmental and engineering geophysics*, Cambridge University Press, Cambridge.
- Stagg, H.M.J., 1985. The structure and origin of Prydz Bay and MacRobertson Shelf, East Antarctica, *Tectonophysics*, **114**, 315–340.
- Sugden, D.E. & John, J.S., 1976. *Glaciers and landscape*, p. 376, Edward Arnold Ltd., London.
- Sweat, M.J., 1997. Continuous seismic-reflection profiling near Grassy Island, Wyandotte Unit of Shiawassee National Wildlife Refuge, Wyandotte, Michigan. USGS Administrative Completion Report for WRD Reimbursable Agreement No. 8-4426-06000 of USFWS Parent Project No. 14-48-0003-97-905, DCN#1448-30181-97-N344, Unofficial publication #ACR97-01, Lansing, Michigan. Web address: <http://mi.water.usgs.gov/pubs/MISC/ACR97-01/ACR97-01LW.php> (accessed 10/06/05)
- Thiel, E. & Ostenso, N.A., 1961. Seismic studies on Antarctic ice shelves, *Geophysics*, **26**(6), 706–715.
- Tingey, R.J., 1972. Geological work in Antarctica, 1971. *Record of Bureau of Mineral Resources, Geology & Geophysics, Australia*. 1972/132, 49 p.
- Tingey, R.J., 1982. The geologic evolution of the Prince Charles Mountains—an Antarctic cratonic block, in *Antarctic Geoscience*, pp. 455–464, ed. Craddock, C., University of Wisconsin Press, Madison, Wisconsin.
- Zelt, C.A. & Smith, R.B., 1992. Seismic traveltime inversion for 2-D crustal velocity structure, *Geophys. J. Int.*, **108**, 16–34.